This paper was originally published as an *ASHRAE Transactions paper* and may be cited as:

Cimmino, M. and M. Bernier. 2014. Effects of unequal borehole spacing on the required borehole length, ASHRAE Transactions, 120(2):158-173.

SE-14-013

Effects of Unequal Borehole Spacing on the Required Borehole Length

Massimo Cimmino
Student Member ASHRAE

Michel Bernier, PhD, PEng
Member ASHRAE

ABSTRACT

The aim of this paper is to show how the number and positioning of boreholes for a given land surface area can affect the fluid and ground temperature variations and the required borehole length. The methodology uses a g-function generation model and then uses temporal superposition to predict the variation of the fluid and borehole wall temperatures over 20 years of operation of the ground-source heat pump system. The cases of a 3 × 7 and 5 × 10 bore field are studied. Results show that the position of boreholes within a bore field of constant land area affects only slightly the required borehole length, while the number of boreholes has a greater, albeit small, impact on the required length. For instance, for the 5 × 10 bore field, the total required borehole length increases by 0.9% when boreholes are displaced towards the center and decreases by 2% when the field was changed to a 5 × 9 configuration. In the latter case, the length of individual boreholes increased by 8.8%.

INTRODUCTION

The design of a geothermal bore field consists in determining the number and length of boreholes required for the ground and heat transfer fluid temperatures to stay within an acceptable range. The temperature of the heat transfer fluid should not drop below a minimum fluid temperature, $T_{f,\min}$, or rise above a maximum fluid temperature, $T_{f,\max}$, to ensure proper heat pump operation. As a result of the extraction and injection of heat from and into the ground, the ground temperature varies during the operation of the ground-source heat pump (GSHP) system. If the building loads are unbalanced, for example, if more heat is extracted than injected during one full year, the temperature of the ground—and that of the fluid—will decrease from one year to the next. This decrease (or increase in the case where more heat is injected than extracted) may lead to unacceptable ground temperature to ensure proper heat transfer from the ground to the fluid.

Typical bore field configurations consist of equally spaced boreholes on a rectangular grid. One such configuration is shown in Figure 1 for a field of six boreholes arranged on two rows.

In a bore field, a portion of the fluid temperature variation is associated with thermal interactions among boreholes. Thermal interactions depend on the size, number, and position of the boreholes within the bore field. Different bore field configurations respond differently to the extraction and injection of heat into the ground, and, thus, the required length of the boreholes differs between configurations.

The aim of this paper is to show how the number and positioning of boreholes for a given land surface area can affect the temperature variations and result in a variation of the required borehole length. The methodology uses the g-function generation model of Cimmino et al. (2013) to predict the variation of the borehole wall temperature and the temperature of the fluid exiting the bore field.

The methodology is applied to simulate two different bore fields: 3 × 7 and 5 × 10 equally spaced boreholes. A 20-year simulation of the bore fields is done using an unbalanced annual heat extraction profile. The required length of each bore field is identified. Then, the number and position of boreholes in the two fields are varied to study their effect on the g-function and on the required borehole length.

Massimo Cimmino is a PhD candidate and **Michel Bernier** is a professor in the Mechanical Engineering Department, Polytechnique Montreal, Quebec, Canada.

LITERATURE REVIEW

Thermal Response Factors

Eskilson (1987) obtained thermal response factors for bore fields by solving the heat transfer between the boreholes and the ground using a finite difference approach. A number of ground heat exchanger design tools and energy simulation programs (e.g., EED [Hellström and Sanner 1994], GLHEPRO [Spitler 2000], EnergyPlus [Fisher et al. 2006], eQUEST [Liu and Hellstrom 2006]) use these g-functions to simulate the transient heat transfer between the boreholes and the ground. Values of g-functions for a number of bore field configurations are included within databases in each simulation program. Since the user has to choose among the provided bore fields, which consist of equally spaced boreholes, the use of these tools restricts the design possibilities to those bore fields.

With the g-function approach, each borehole is modeled in a 2-D radial-axial mesh. At each time step, the temperature distribution around every borehole is superposed to obtain the total temperature distribution in the bore field. The method of images is used to account for the constant ground surface temperature. The uniform borehole wall temperature (same for all boreholes) required to maintain the constant total heat extraction rate is then calculated. The temperature distribution at the end of each time step is calculated by forward-explicit finite differences. The resulting response factors, called g-functions, give the nondimensional borehole wall temperature drop due to a constant unit heat extraction rate at the borehole walls. According to Eskilson (1987), g-functions are defined by the following:

$$T_b = T_g - (Q'_g/2\pi k_s) \cdot g(t/t_s, r_b/H, B/H) \quad (1)$$

where T_b is the borehole wall temperature, T_g is the undisturbed ground temperature, Q'_g is the heat extraction rate per unit length of borehole, k_s is the ground thermal conductivity, t/t_s is the nondimensional time with $t_s = H^2/9\alpha_s$ the characteristic time, H is the length of an individual borehole, α_s is the ground thermal diffusivity, r_b is the borehole radius, and B is the spacing between two adjacent boreholes. g-functions give a direct relation between the heat extraction rate in the bore field and the temperature variation at the borehole walls: the greater is the value of the g-function, the greater is the temperature variation at the borehole walls for a given heat extraction rate. For $Q'_g/2\pi k_s = 1$, the variation of the borehole wall temperature is equal to the g-function of the bore field. Values of g-functions for a field of 3 × 2 boreholes are shown in Figure 2. They are usually presented for a ratio $r_b/H = 0.0005$ and for various values of the B/H ratio. A ratio $B/H = \infty$ corresponds to the case of a single borehole.

Thermal response factors for bore fields can also be obtained using analytical solutions. Ingersoll and Plass (1948) and Ingersoll et al. (1950, 1954) used both Kelvin's infinite line source (ILS) solution and the cylindrical heat source

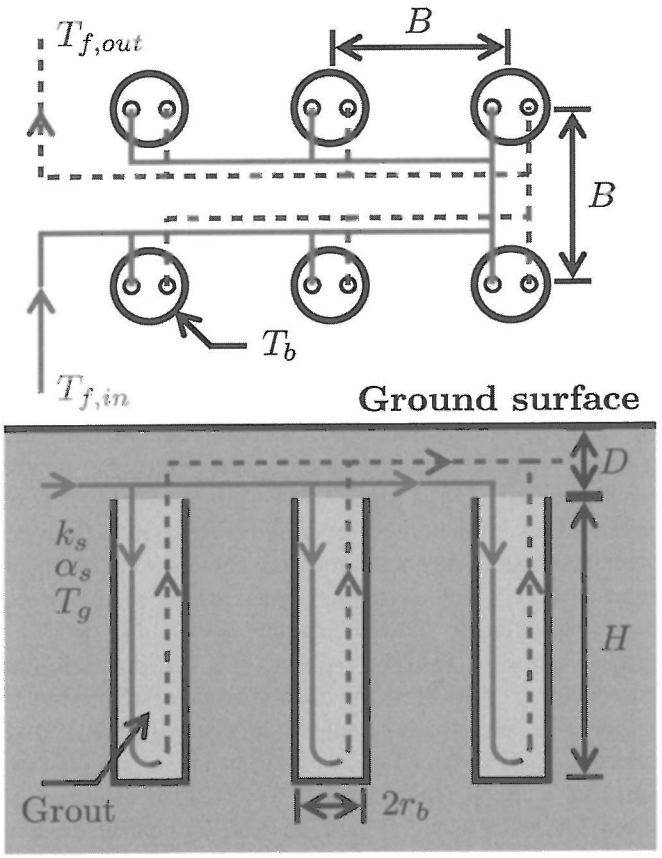

Figure 1 *Field of 3 × 2 equally spaced boreholes arranged in a parallel configuration.*

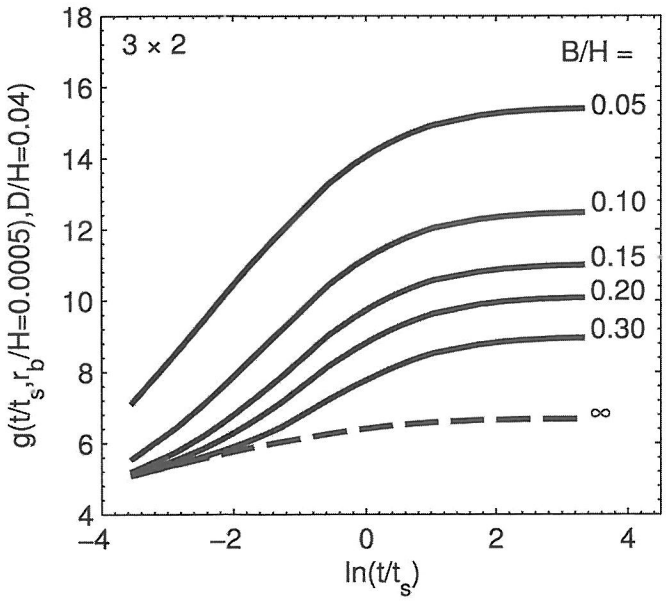

Figure 2 *g-functions of a field of 3 × 2 boreholes.*

(CHS) solution from Carslaw and Jaeger (1946) to obtain the variation of temperature near boreholes. Analytical solutions are superposed in space and time to account for thermal interaction between boreholes and time-varying heat extraction rates. Eskilson (1987) proposed the finite line source (FLS) for the approximation of the g-functions. The solution is obtained by the spatial superposition of point heat sources over the length of the borehole:

$$T(r,z,t) = T_g - Q'/4\pi k_s \cdot \int_D^{H+D} \left[\frac{erfc\left(\frac{\sqrt{r^2+(z-s)^2}}{\sqrt{4\alpha_s t}}\right)}{\sqrt{r^2+(z-s)^2}} - \frac{erfc\left(\frac{\sqrt{r^2+(z+s)^2}}{\sqrt{4\alpha_s t}}\right)}{\sqrt{r^2+(z+s)^2}} \right] ds \quad (2)$$

where D is the buried depth of the borehole and *erfc* is the complementary error function. Eskilson obtained the borehole wall temperature by evaluating the FLS solution at midlength ($z = D + H/2$) and at a radius $r = \sqrt{1.5} r_b$ corresponding to the radius of an ellipsoid having the same volume as the borehole because the isotherms around a finite line source tend to resemble slightly distorted ellipsoids.

The FLS was latter reintroduced by Zeng et al. (2002) who evaluated the solution at midlength and at the borehole radius to obtain the temperature at the borehole wall. The temperature at midlength was chosen instead of the average temperature over the length of the borehole to avoid solving a double integral. Lamarche and Beauchamp (2007a) obtained a solution for the average temperature over the length of the borehole by simplifying the FLS for a buried depth, $D = 0$. Claesson and Javed (2011) obtained a solution for $D \geq 0$ which gives the average temperature over the length of the borehole:

$$\bar{T}(r,t) = T_g - \frac{Q'}{4\pi k_s} \cdot \int_{1/\sqrt{4\alpha_s t}}^{\infty} \exp(-r^2 s^2) \cdot \frac{Y(Hs, Ds)}{Hs^2} \cdot ds \quad (3)$$

$$Y(h,d) = 2 \cdot ierf(h) + 2 \cdot ierf(h+2d) - ierf(2h+2d) - ierf(2d) \quad (4)$$

$$ierf(X) = X \cdot erf(X) - \frac{1}{\sqrt{\pi}}[1 - \exp(-X^2)] \quad (5)$$

where $\bar{T}$ is the average temperature over the length of the borehole at a distance r from its center, and *erf* is the error function. The FLS solution can be expressed in the form of a response factor, according to the definition of the g-function (Equation 2):

$$h_{FLS}(t, r, H, D) = \frac{1}{2} \cdot \int_{1/\sqrt{4\alpha_s t}}^{\infty} \exp(-r^2 s^2) \cdot \frac{Y(Hs, Ds)}{Hs^2} \cdot ds \quad (6)$$

where h_{FLS} is the borehole-to-borehole response factor.

The thermal response factor of a bore field can be obtained by the spatial superposition of the FLS solution, assuming that all boreholes have the same heat extraction rate. The thermal response factor is given by the average temperature variation of every borehole in the field:

$$g_{FLS}(t) = \frac{1}{N_b} \sum_{i=1}^{N_b} \sum_{j=1}^{N_b} h_{FLS}(t, d_{ij}, H, D) \quad (7)$$

$$d_{ij} = \begin{cases} r_b & \text{for } i = j \\ \sqrt{(x_i - x_j)^2 + (y_i - y_j)^2} & \text{for } i \neq j \end{cases} \quad (8)$$

where g_{FLS} is the thermal response factor for the bore field obtained using what is referred to here as classical superposition of the FLS, N_b is the number of boreholes in the field and $(x_i y_i)$ are the coordinates of the ith borehole.

Fossa (2011) compared the thermal response factors obtained using the classical superposition of the FLS (Equation 7) with Eskilson's g-functions. The author noted that, for small values of the spacing to length ratio B/H and for large values of the nondimensional time t/t_s, the classical superposition of the FLS overestimated Eskilson's g-functions.

Cimmino et al. (2013) used the FLS solution to generate g-functions while accounting for the variation of the heat extraction rates among boreholes. The authors accounted for thermal interaction among boreholes by imposing an average borehole wall temperature equal for all boreholes. Spatial and temporal superpositions are used to obtain a linear system of equation in the Laplace domain. The solution to the system of equations gives the normalized heat extraction rates of every borehole as well as the nondimensional borehole wall temperature, which corresponds to the thermal response factor of the bore field. Results showed that the model gives a better approximation of Eskilson's g-functions than the classical superposition of the FLS. The method was recently improved to apply to fields of boreholes of unequal lengths and to consider a boundary condition of uniform temperature at the borehole walls (Cimmino and Bernier 2014). The results showed that Eskilson's g-functions can be replicated accurately. The authors developed a software tool that generates g-functions based on user inputs of borehole dimensions and positions (Cimmino and Bernier 2013).

Simulation Using Thermal Response Factors

The variation of the borehole wall temperature can be obtained through the temporal superposition of the thermal response factor:

$$T_b(t_k) = T_g - \sum_{i=1}^{k} \left\{ \frac{q'(t_i)}{2\pi k_s} \cdot g[(t_k - t_{i-1})/t_s, r_b/H, B/H] \right\} \quad (9)$$

where $q'(t_i) = Q'(t_i) - Q'(t_{i-1})$ is the heat extraction rate increment per unit borehole length, $t_i - t_{i-1} = \Delta t$ the simulation time step, and $q'(t_1) = Q'(t_1)$. Equation 9 is also known as the temporal superposition of loads. As the number of simulation time steps increases, the number of terms in the sum of Equation 9 becomes larger and the temporal superposition of loads is increasingly long to compute.

Methods have been proposed by several authors to reduce the calculation time associated with temporal superposition. For instance, Yavuzturk and Spitler (1999) introduced load aggregation. The method consists in averaging the loads for times prior to $t^* = t_k - n_{ag} \cdot \Delta t$, where n_{ag} is the number of nonaggregated time steps. The number of terms in the summation of Equation 9 is then inferior or equal to $n_{ag}+1$. This greatly reduces the number of terms in the summation and thereby reduces the time required for the simulation. The authors reduced the time required for a 20-year hourly simulation by 99%.

Bernier et al. (2004) improved the method of aggregation of loads by defining multiple aggregation groups. The multiple load aggregation algorithm (MLAA) consists in grouping the loads to be averaged in several groups, including a larger number of time steps as the time steps are farther away from t_k. Five groups are defined: the nonaggregated hourly loads and the daily, weekly, monthly, and yearly loads. Optimization of the group sizes was done in order to maximize the precision of the temporal superposition of loads for a given calculation time.

A similar algorithm for the aggregation of loads was developed by Liu (2005) and referred to as the "hierarchical load aggregation procedure." The hourly loads are grouped into a number of small, medium, and large aggregation blocks. While the size of each block is set, the number of blocks of each size is adapted at each time step according to the length of the load history. The algorithm is used in EnergyPlus for the simulation of GSHP systems.

Lamarche and Beauchamp (2007b) proposed a nonhistory dependent algorithm for the temporal superposition of loads. The authors expressed the temporal superposition of the CHS solution in the form of a Green function. By inverting the order of integration, the temperature at the last time step can be obtained using only the ground load at the last time step and the solution from the previous time step. The authors obtained a simulation time of 1.39 s for a two-year hourly simulation, whereas the same simulation was done in 25.1 s using the MLAA. Lamarche (2009) later generalized the algorithm to enable the use of any thermal response factor.

Marcotte and Pasquier (2008) noted that the sum of Equation 9 is in fact a convolution product, which can be solved using Fourier transforms. Equation 9 is rewritten as:

$$T_b(t) = T_g - \mathcal{F}^{-1}\left\{ \mathcal{F}\left[\frac{q'(t)}{2\pi k_s}\right] \cdot \mathcal{F}[g(t/t_s, r_b/H, B/H)] \right\} \quad (10)$$

where $\mathcal{F}$ and $\mathcal{F}^{-1}$ are the direct and inverse Fourier transforms.

The authors also proposed to subsample the evaluation of the FLS and interpolated the solution in order to obtain the FLS solution for all time steps of the simulation. Using a fast Fourier transform (FFT) algorithm and a cubic spline interpolant, the authors were able to achieve a 20-year simulation with an hourly time step for a field of 40 boreholes in less than a minute on a typical desktop computer. Cimmino et al. (2012) showed how the FFT can be used to simulate GSHP systems with g-functions. The simulation time for a 20-year simulation with an hourly time step for a field of 3 × 6 boreholes was reduced by three orders of magnitude compared to a simulation performed using the MLAA.

Optimization of Bore Field Geometry

Bore field optimization is rarely seen in ground heat exchanger design tools. Most design software tools serve the purpose of determining the required borehole length based on a bore field geometry given by the user. One exception is the latest version of EED (Blomberg et al. 2008), which provides an optimization tool to find the best bore field configuration based on the required borehole length or the total cost. The software does successive simulation of all bore field configurations that fit into the specified available land area, varying the spacing between boreholes for each configuration. The available fields are, however, restricted to bore fields with evenly spaced boreholes. Another example is the program EWS (Huber 2011), which lets the user input custom borehole positions in order to calculate a thermal response factor and simulate the bore field.

Beck et al. (2013) studied the effect of the borehole positions in a bore field on the temperature variation of the ground in the bore field. The positions of boreholes in a field of 36 boreholes on a 6 × 6 grid were varied and the ground temperatures were obtained from the simulation of the bore field using a given monthly variation of the heat extraction rates over 30 years. It was shown that positioning the boreholes on the perimeter of the field resulted in a lower temperature drop in the ground.

Kurevija et al. (2012) compared the cylindrical heat source solution and Eskilson's g-function for the simulation and sizing of a 7 × 6 and a 21 × 2 bore fields using a heating-dominated load profile. It was shown that the required length obtained from the use of the CHS solution is greater than that calculated using Eskilson's g-functions. Additionally, the 21 × 2 bore field resulted in smaller fluid and ground temper-

ature drops, and thus the 21 × 2 bore field achieved a smaller required borehole length than the 7 × 6 bore field. It was noted that thermal interactions are more important for more compact fields, in this case the 7 × 6 bore field.

Robert and Gosselin (2014) presented an optimization methodology for the total cost minimization of ground coupled heat pump systems. Optimization variables included the borehole length, the number and geometric configuration of boreholes on a rectangular grid, the spacing between boreholes, and the portion of the building load assumed by the geothermal system. The authors demonstrated that the total cost is most importantly influenced by the length and number of boreholes. The uncertainty on the value of the ground thermal conductivity and the cost related with the evaluation of the thermal conductivity via thermal response tests (TRT) were also studied by the authors. It was shown that the evaluation of the ground thermal conductivity is mostly important when the thermal conductivity is low and the number of boreholes in the bore field is high.

PROPOSED METHODOLOGY

The model proposed by Cimmino et al. (2013) is used to generate g-functions for the simulation and sizing of two bore fields. The base configuration of the two bore fields consists of 21 equally spaced boreholes on a rectangular 3 × 7 grid and 50 equally spaced boreholes on a rectangular 5 × 10 grid, as shown in Figure 3. The 3 × 7 bore field was selected based on the ground loads obtained for this study, as shown in Figure 4. The 5 × 10 bore field was included to validate that the results apply to larger bore fields. However, the methodology applies to other configurations and will be used to study variations of the two bore fields. Boreholes have a radius r_b, a length H, and are buried at a depth D. The ground has a thermal conductivity k_s, a thermal diffusivity α_s and is initially at a temperature T_g. The ground surface is maintained at the initial ground temperature T_g.

Boreholes are modeled as finite line sources with a uniform heat extraction rate over their entire length. The total heat extraction rate is constant, but individual boreholes may have different heat extraction rates. The average over-the-length borehole wall temperature is assumed to be equal for every borehole in the field in accordance with Eskilson's g-function definition. This assumption is used to model the operation of boreholes connected in parallel. An equal borehole wall temperature for every borehole is justified, provided that the inlet fluid temperature is equal for all boreholes and the temperature difference between inlet and outlet is small. In that case, the temperature at the borehole walls should tend to the same value. The condition of equal borehole wall temperature differs from the condition typically used when modelling boreholes using analytical heat source solutions, which is the condition of a uniform heat extraction rate equal for all boreholes.

Temporal Superposition

The temperature variation at the wall of a borehole caused by the extraction of heat at another borehole is obtained by the temporal superposition of the borehole-to-borehole response factors:

$$\Delta T_{i \to j}(t_k) = - \sum_{p=1}^{k} \left\{ \frac{q'_i(t_p)}{2\pi k_s} \cdot h_{i \to j}(t_k - t_{p-1}) \right\} \tag{11}$$

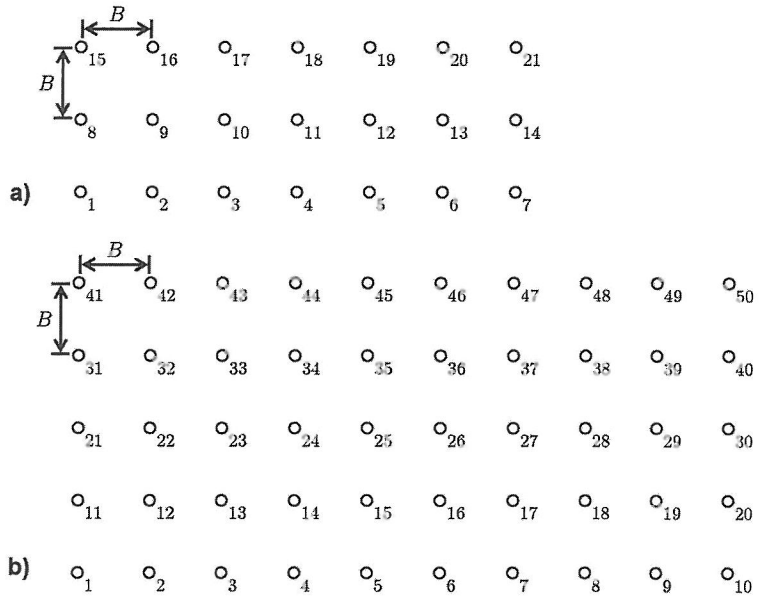

Figure 3 *Identification of the boreholes in (a) 3 × 7 bore field and (b) 5 × 10 bore field.*

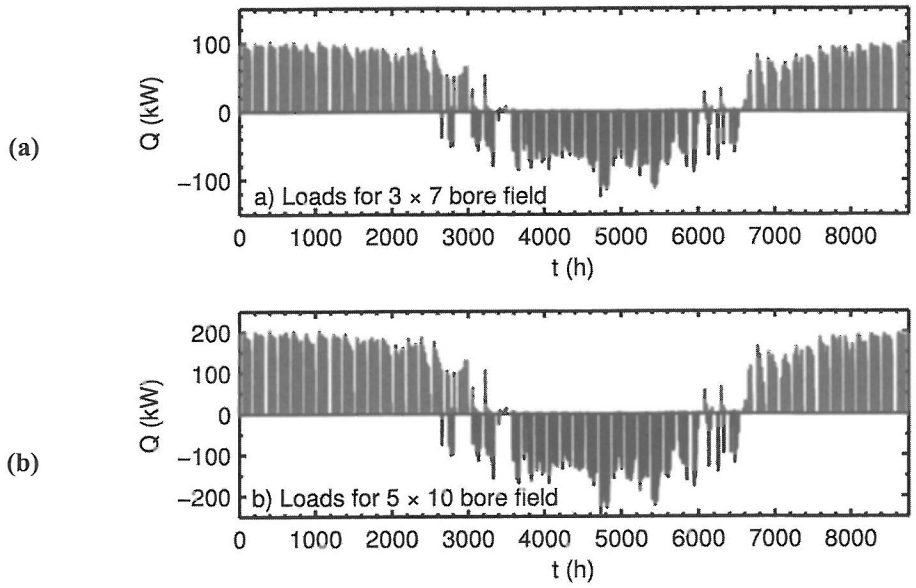

Figure 4 *Ground loads for (a) the 3 × 7 bore field and (b) the 5 × 10 bore field.*

$$h_{i \to j}(t) = h_{FLS}(t, d_{ij}, H, D) \tag{12}$$

$$d_{ij} = \begin{cases} r_b & \text{for } i = j \\ \sqrt{(x_i - x_j)^2 + (y_i - y_j)^2} & \text{for } u \neq j \end{cases} \tag{13}$$

where $\Delta T_{i \to j}$ is the temperature variation at the wall of borehole j, caused by the extraction of heat from borehole i; q_i' is the heat extraction rate increment per unit length of borehole i; and (x_i, y_i) are the coordinates of borehole i. $h_{i \to j}$ is the borehole-to-borehole response factor from borehole i to borehole j.

Spatial Superposition

The total temperature variation at the borehole walls is obtained by the sum of the temperature variations caused by every borehole:

$$\Delta T_b(t_k) = -\sum_{p=1}^{k} \sum_{i=1}^{N_b} \left[\frac{q'_i(t_p)}{2\pi k_s} \cdot h_{i \to j}(t_k - t_{p-1}) \right] \tag{14}$$

where $\Delta T_b = T_b - T_g$ is the temperature variation at the borehole wall (same for all boreholes) and N_b is the number of boreholes in the bore field. Equation 14 can be evaluated for any borehole j to create a set of N_b equations with N_b+1 unknowns (q_i' and ΔT_b). One last equation is required to complete the set. This last equation states that the sum of the heat extraction rate increments is equal to the ground load increment:

$$q_g(t_k) = \sum_{i=1}^{N_b} [H \cdot q_i'(t_k)] \tag{15}$$

where $q_g(t_k) = Q_g(t_k) - Q_g(t_{k-1})$ is the ground load increment and Q_g is the ground load.

System of Equation in the Laplace Domain

The complete set of equations (Equations 14 and 15) is, however, difficult to solve due to the sum involving the time variable in Equation 14. The set of equations can be turned into a simple system of linear equations using Laplace transforms. As noted by Marcotte and Pasquier (2009), the summation in the time domain in Equation 14 is in fact a convolution product and can be replaced by a simple multiplication in the spectral domain. The Laplace transform is used here to avoid temporal aliasing, which would occur when solving the system of equation using Fourier transforms. The Laplace transform pairs are expressed as:

$$F(s) = \mathcal{L}[f(t)] = \int_0^\infty f(t)\exp(-st)dt \tag{16}$$

$$f(t) = \mathcal{L}^{-1}[F(s)] = \frac{1}{2\pi j}\int_{\sigma - j\infty}^{\sigma + j\infty} F(s)\exp(st)ds \tag{17}$$

where $\mathcal{L}$ and $\mathcal{L}^{-1}$ are the direct and inverse Laplace transforms, f is an arbitrary function in the time domain, F is the corresponding function in the Laplace domain, s is the complex frequency in the Laplace domain, and $j = \sqrt{-1}$ is the imaginary number.

By imposing a variable change $s = \sigma + j\omega$ (Moreno and Ramirez 2008), the Laplace transform can be obtained from the Fourier transform:

$$F(s) = \int_0^{\infty} [f(t)\exp(-\sigma t)]\exp(-j\omega t)dt = \mathcal{F}[h(t)\cdot\exp(-\sigma t)] \quad (18)$$

$$f(t) = \frac{\exp(\sigma t)}{2\pi}\int_{-\infty}^{+\infty} F(s)\exp(j\omega t)d\omega = \exp(\sigma t)\cdot\mathcal{F}^{-1}[H(s)] \quad (19)$$

where ω is the angular frequency in the Fourier domain and σ is a real positive constant. The value of σ should be large enough to avoid temporal aliasing and small enough to avoid distorting the results. The value of σ is chosen according to Wedepohl's criterion (Wedepohl 1983):

$$\sigma = 2\cdot\frac{\ln(N)}{t_{max}} \quad (20)$$

where N is the number of time steps in the simulation and t_{max} is the maximum value of the time variable.

Equation 14 and 15 are expressed in the Laplace domain:

$$\mathcal{L}(\Delta T_b) = -\sum_{i=1}^{N_b}\left[\mathcal{L}\left(\frac{q'_i}{2\pi k_s}\right)\cdot\mathcal{L}(h_{i\to j})\right] \quad (21)$$

$$\mathcal{L}(q_g) = \sum_{i=1}^{N_b}[H\cdot\mathcal{L}(q'_i)] \quad (22)$$

Equations 21 and 22 form a system of $N_b + 1$ linear equations, which can be written in matrix form:

$$\begin{bmatrix} 0 \\ \vdots \\ 0 \\ 0 \\ \mathcal{L}\left(\frac{-q_g}{2\pi k_s H}\right) \end{bmatrix} =$$

$$\begin{bmatrix} \mathcal{L}h_{1\to 1} & \cdots & \mathcal{L}(h_{(N_b\to 1)\to 1}) & \mathcal{L}(h_{N_b\to 1}) & -1 \\ \vdots & \ddots & \vdots & \vdots & \vdots \\ \mathcal{L}h_{1\to(N_b-1)} & \cdots & \mathcal{L}(h_{(N_b-1)\to(N_b-1)}) & \mathcal{L}(h_{N_b\to(N_b-1)}) & -1 \\ \mathcal{L}(h_{1\to N_b}) & \cdots & \mathcal{L}(h_{(N_b-1)\to N_b}) & \mathcal{L}(h_{N_b\to N_b}) & -1 \\ 1 & \cdots & 1 & 1 & 0 \end{bmatrix}$$

$$\begin{bmatrix} \mathcal{L}\left(\frac{-q'_1}{2\pi k_s}\right) \\ \vdots \\ \mathcal{L}\left(\frac{-q'_{N_b-1}}{2\pi k_s}\right) \\ \mathcal{L}\left(\frac{-q'_{N_b}}{2\pi k_s}\right) \\ \mathcal{L}(\Delta T_b) \end{bmatrix} \quad (23)$$

The system of equations is solved for each term of the Laplace transforms. The solution of the system gives the variation of the borehole wall temperature and the heat extraction rates for each borehole.

APPLICATION

The methodology presented above is used to study borehole positioning in two bore fields over a period of 20 years. The first bore field consists of 21 boreholes on 3 rows, namely the 3 × 7 bore field, and the second bore field consists of 50 boreholes on 5 rows, namely the 5 × 10 bore field.

Ground loads for the 3 × 7 bore field are obtained from the simulation of a two-story office building located in Montreal, Quebec, using eQUEST. Ground loads are obtained from the building heating and cooling loads, which are weighted to account for heat pump efficiency in heating and cooling. The hourly ground loads are shown in Figure 4a; heat extracted from the ground is shown as positive. The ground loads are heating dominated (i.e., more heat is extracted than injected into the ground on an annual basis). Ground loads for the 5 × 10 bore field are obtained from the loads of the 3 × 7 bore field, which are multiplied by a factor of 2. The hourly ground loads are shown in Figure 4b. The peak heat extraction and heat injection rates, the total heat extracted and injected during one year, and the yearly average heat extraction rate are shown in Table 1.

For both cases, the bore fields consist of boreholes on a rectangular grid with a spacing B = 7 m (23 ft). Boreholes are buried at a distance D = 2 m (6.5 ft) from the ground surface, have a radius r_b = 0.075 m (3 in.), and have a thermal resistance R_b = 0.1 m·K/W (0.0144 h·ft²·°F/Btu·in.). Boreholes are connected in parallel. The total fluid flow rate in the bore field is $\dot{m}$ = 7 L/s (111 gpm) for the 3 × 7 bore field and $\dot{m}$ = 16 L/s (254 gpm) for the 5 × 10 bore field. The fluid has a density of ρ = 1015 kg/m³ (63.4 lb/ft³) and a thermal capacity of c_p = 3.97 kJ/kg·K (0.948 Btu/lb·°F). The thermal

Table 1. Peak, Total, and Average Ground Heat Transfer Rates for the 3 × 7 and 5 × 10 Bore Field

	3 × 7 Bore Field	5 × 10 Bore Field
Peak heat extraction rate, kW (kBtu/h)	100.8 (344)	201.3 (687)
Peak heat injection rate, kW (kBtu/h)	123.2 (420)	246.4 (841)
Total heat extracted, kWh (MBtu)	86,993 (297)	173,986 (594)
Total heat injected, kWh (MBtu)	46,115 (157.4)	92,230 (315)
Average heat extraction rate imbalance, kW (kBtu/h)	4.67 (15.93)	9.34 (31.9)

conductivity of the ground is k_s = 2 W/m·K (1.16 Btu/h·ft·°F) and the thermal diffusivity of the ground is $\alpha_s = 1 \times 10^6$ m^2/s (1.08×10^5 ft^2/s). The ground is initially at a temperature T_g = 10°C (50°F).

Bore Field Sizing

The fluid temperature at the outlet of the bore field is obtained from the borehole wall temperature, assuming a linear variation of the fluid temperature inside the boreholes:

$$T_{f,\,\mathrm{out}}(t) = T_b(t) - \frac{Q_g(t)}{N_b \cdot H} R_b + \frac{Q_g(t)}{2\dot{m}c_p} \qquad (24)$$

The borehole wall temperature is obtained from the temporal superposition of the g-function (Equation 9). For both bore fields, the minimum borehole length required to have a minimum outlet fluid temperature of 0°C (32°F) is identified. The fluid temperature variations obtained from the 20 years of hourly simulations for both fields are shown in Figure 5. For the 3 × 7 bore field, the minimum required borehole length is 121 m (397 ft). As shown in Figure 5a, the minimum fluid temperature is attained after 20 years. Since the ground loads are heating dominated, the fluid temperature gets lower from year to year. For the 5 × 10 bore field, the minimum borehole length is 113 m (371 ft). As was the case for the 3 × 7 bore field, Figure 5b shows that the minimum fluid temperature is attained after 20 years.

BORE FIELD OPTIMIZATION

Two strategies are examined to reduce the required borehole length in the bore fields, given the same land area. The first strategy consists in displacing the boreholes in the bore fields, either away from or towards the center of the field. The second strategy consists in removing or adding boreholes to the bore field. Each strategy is first compared with the base bore fields using their respective g-functions. The effect of the change in bore field configuration on the required borehole length is then studied.

Displacing Boreholes in the Bore Field

Previous studies have shown that the boreholes located near the center of the field tend to extract less heat over time due to the fact that the temperature in the center of the bore field drops faster than on the perimeter of the field. It may then be advantageous to use unequal borehole spacing to reduce the total required borehole length. As was the case above, the bore fields consist of 21 boreholes distributed on 3 rows and 50 boreholes distributed on 5 rows. However, in contrast to the bore fields studied in the previous section, the spacing between two adjacent boreholes on the same row varies. Unequal borehole spacing in the other perpendicular direction could also be envisioned with the proposed methodology. However, in the present case, only the borehole spacing in one direction is varied. These new bore field configurations are shown in Figure 6. The bore field occupies the same land area as the bore fields shown in Figure 3 and the average spacing between two adjacent boreholes on the same row is thus B = 7 m (23 ft). The spacing between boreholes grows with a factor f_i towards the center of the bore field.

The g-function of the base field of 21 boreholes is compared to a bore field where boreholes are displaced away the center of the bore field, with B_1 = 3 m (9.8 ft), B_2 = 5 m (16.4 ft), f_1 = 2, and f_2 = 1.36; and to a bore field where boreholes are displaced towards the center of the bore field, with B_1 = 12 m (39 ft), B_2 = 9.2 m (30 ft), f_1 = 0.5, and f_2 = 0.74. The g-functions are compared in Figure 7, for a common

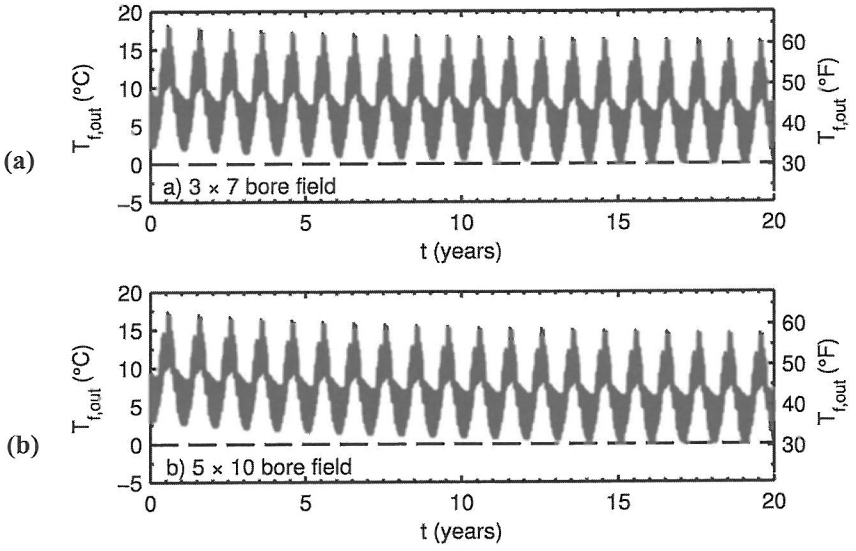

Figure 5 *Variation of the outlet fluid temperature for (a) the 3 × 7 bore field and (b) the 5 × 10 bore field.*

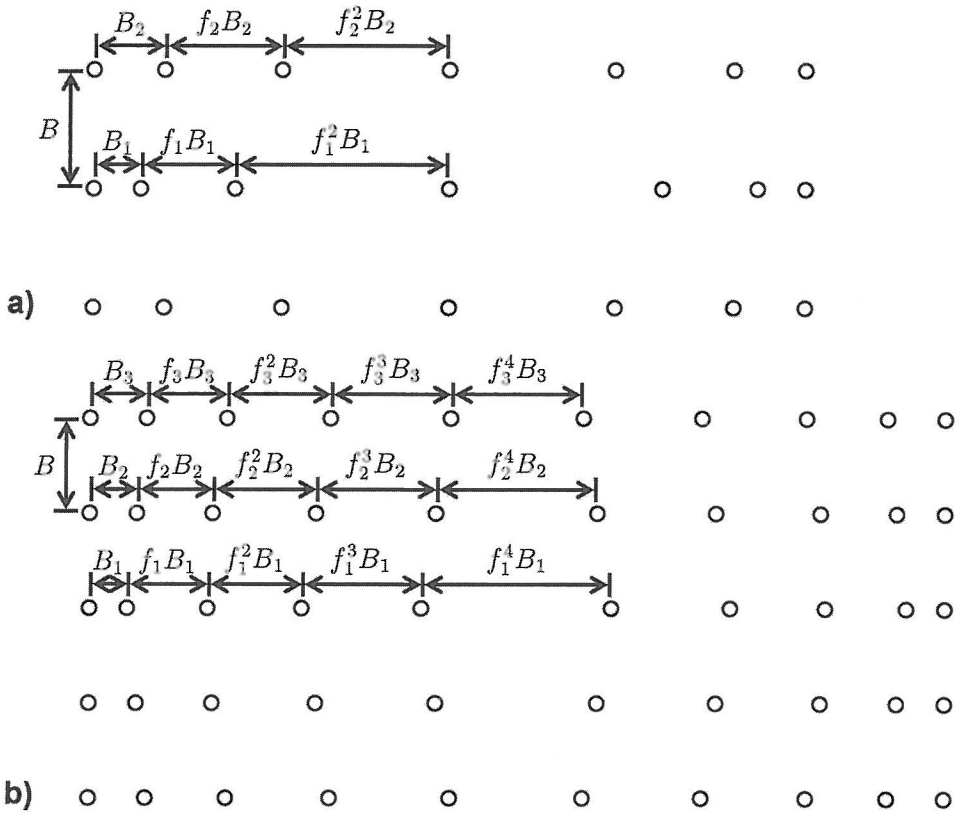

Figure 6 *Fields of (a) 3 × 7 and (b) 5 × 10 unevenly spaced boreholes.*

length $H = 121$ m. It is shown that the impact of the changes on the g-function is negligible. This means that the borehole wall temperature response is about the same for each configuration. For example, after 20 years (i.e., for $\ln[t/t_s] = -0.95$) the g-functions show a difference of –0.56% and 1.65% with the base field when the boreholes are displaced away from the center of the field and towards the center of the field, respectively. The impact on the required borehole length is also relatively very small: the required borehole length for the field with the boreholes displaced away from the center is $H = 121$ m (397 ft) (same as the equally spaced bore field), and the required borehole length for the field with the boreholes displaced towards the center is $H = 122$ m (400 ft).

The same comparison is made for the field of 50 boreholes. The base configuration is compared to a bore field with the boreholes displaced away from the center, with $B_1 = 3$ m (9.8 ft), $B_2 = 4.5$ m (14.8 ft), $B_3 = 6$ m (19.7 ft), $f_1 = 1.49$, $f_2 = 1.25$, and $f_3 = 1.09$ and to a bore field with the boreholes displaced towards the center, with $B_1 = 11.6$ m (38 ft), $B_2 = 9.46$ m (31 ft), $B_3 = 7.86$ m (26 ft), $f_1 = 0.71$, $f_2 = 0.83$, and $f_3 = 0.93$. The g-functions are compared in Figure 8, for a common length $H = 113$ m (371 ft). Once again, the impact of the changes on the g-function is negligible. For example, after 20 years, the difference between the g-function of the field with the boreholes displaced away from the center of the field and the g-function of the base field is –0.48%. The difference between the g-function of the field with the boreholes displaced towards the center of the field and the g-function of the base field is 0.73%. The required lengths are as follows: $H = 113$ m (371 ft) (same as the equally-spaced boreholes) for the field with the boreholes displaced away from the center and $H = 114$ m (374 ft) for the field with the boreholes displaced towards the center.

Removing or Adding Boreholes

The effect of removing and adding boreholes to the bore field is now studied. The 3 × 7 bore field is compared to a 3 × 6 bore field and to a 3 × 8 bore field, with the horizontal spacing B_{hor} adjusted so the bore field occupies the same land area. The horizontal spacing is thus $B_{hor} = 8.4$ m (28 ft) for the 3 × 6 bore field and $B_{hor} = 6.0$ m (19.7 ft) for the 3 × 8 bore field. The g-functions are compared in Figure 9 for the same total borehole length $N_b \cdot H = 2541$ m (8337 ft). The characteristic time t_s is calculated for $H = 121$ m (397 ft) so the nondimensional time axis of the g-function graph is coherent between the 3 bore fields. The 3 × 6 bore field shows a reduction of the g-function while the 3 × 8 bore field shows an increase of the g-function value. The reduction of the g-function is 10.0% at $t = 20$ years for the 3 × 6 bore field. The increase is 9.41% at $t = 20$ years for the 3 × 8 bore field. These variations are

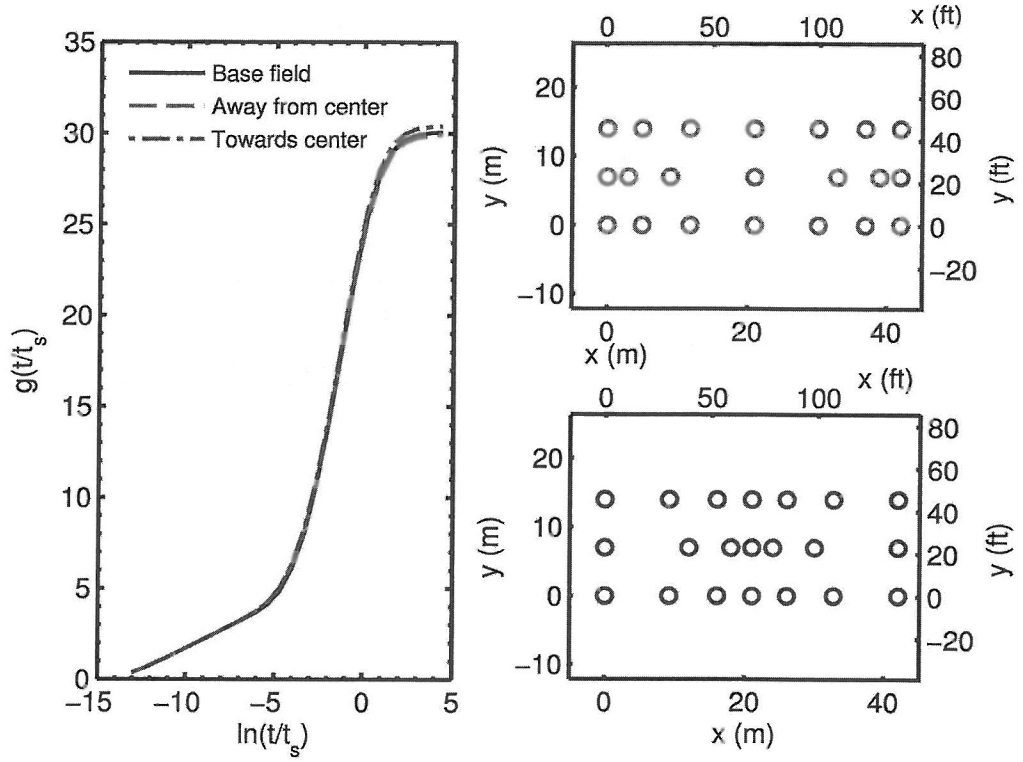

Figure 7 *g-functions of a 3 × 7 bore field with equal and unequal spacing between boreholes.*

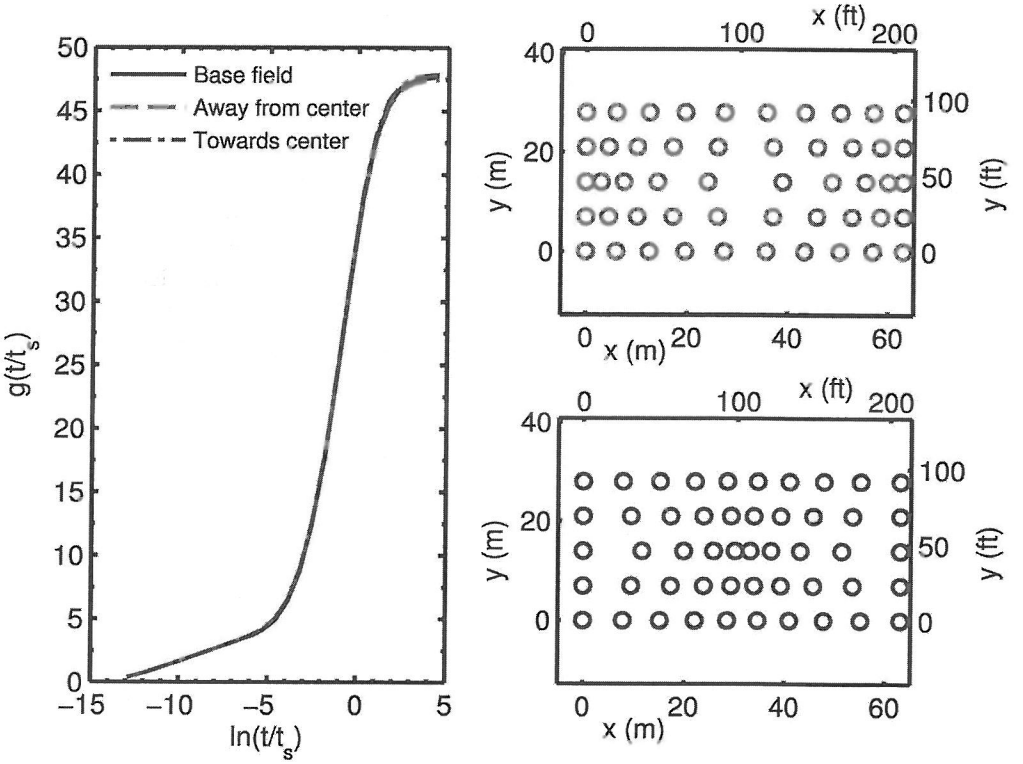

Figure 8 *g-functions of a 5 × 10 bore field with equal and unequal spacing between boreholes.*

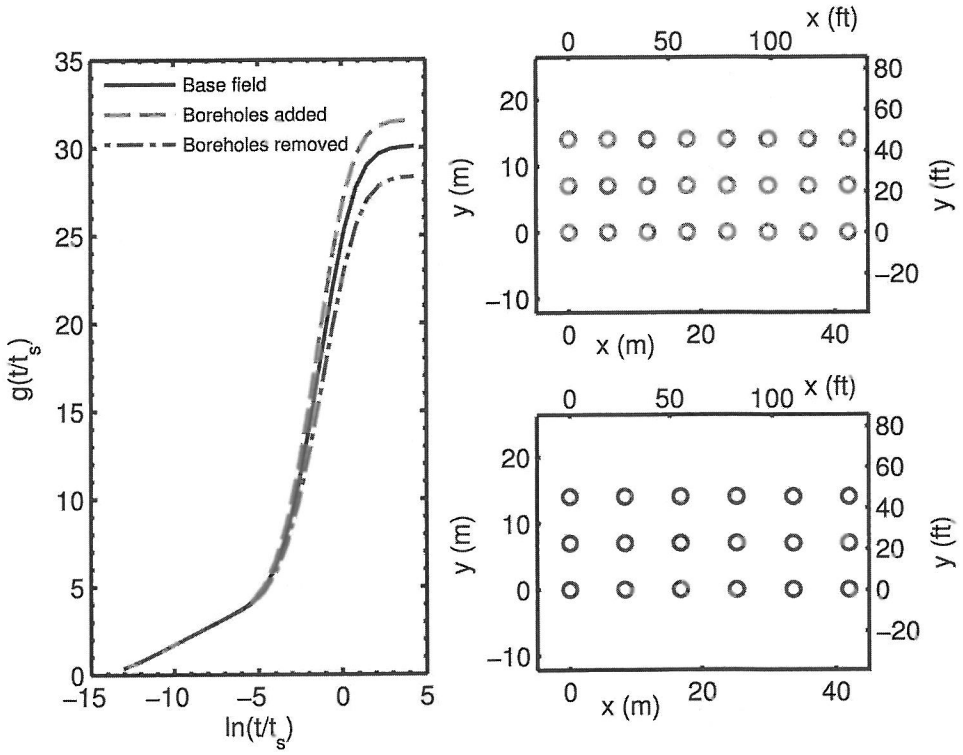

Figure 9 *g-function of a 3 × 7 bore field with compared with the g-functions of a 3 × 8 and a 3 × 6 bore field.*

explained by the fact that an increase in the number of boreholes reduces the distance between boreholes and thereby increase the effect of thermal interactions. Furthermore, an increase in the number of boreholes is accompanied by a decrease in the length of the individual boreholes. The reduction in length effectively reduces the ground volume occupied by the bore field and therefore reduces the ground volume from which the bore field can extract heat. A variation of the required borehole length is expected as a consequence of the changes in the g-function values. Indeed, the required total borehole length is 2484 m (8150 ft) for the 3 × 6 bore field and 2592 m (8504 ft) for the 3 × 8 bore field. The individual borehole lengths are then $H = 138$ m (453 ft) and $H = 108$ m (354 ft), respectively.

The same strategy is used on the 5 × 10 bore field, which is compared to a 5 × 9 bore field and to a 5 × 11 bore field. The horizontal spacing is $B_{hor} = 7.9$ m (26 ft) for the 5 × 9 bore field and $B_{hor} = 6.3$ m (21 ft) for the 5 × 11 bore field. The g-functions are compared in Figure 10 for the same total borehole length $N_b \cdot H = 5650$ m (18537 ft). The characteristic time t_s is calculated for $H = 113$ m (371 ft). The results are similar to the 3 × 7 bore field, as the g-functions are reduced for the field with removed boreholes and increased for the field with added boreholes. The reduction of the g-function is 6.88% at $t = 20$ years for the 5 × 9 bore field. The increase is 6.47% at $t = 20$ years for the 5 × 11 bore field. The required total borehole length is reduced to 5535 m (18,159 ft) for the 5 × 9 bore field and increased to 5775 m (18,947 ft) for the 5 × 11 bore field. The individual borehole lengths are then $H = 123$ m (404 ft) and $H = 105$ m (344 ft), respectively.

The required individual and total borehole lengths are summarized in Table 2 for the two bore fields and each strategy. It is shown that displacing boreholes in the field has relatively little impact on the required borehole length. Results presented here seem to indicate that it is not beneficial to displace boreholes inside the bore field, as it does not decrease the required length. However, small variations of the borehole positions have negligible effects on the required borehole length. This has an important implication for designers and drillers: the positioning of boreholes can be altered, within a given land area, without affecting the performance of the system

Removing boreholes from the bore fields reduces the total required length while adding boreholes increases the total required length. Removing three boreholes from the 3 × 7 bore field reduces the total required length by 2.2% while increasing the individual borehole length by 14.0%. Removing five boreholes from the 5 × 10 bore field reduces the total required length by 2.0%, while increasing the individual borehole length by 8.8%. These values are valid for a borehole resistance of 0.1 m·K/W (0.0144 h·ft^2·°F/Btu·in.). The variation of the required length correlates with the variation of the g-function value: a reduction of the g-function is seen in cases where the required length is reduced, as shown in Table 3.

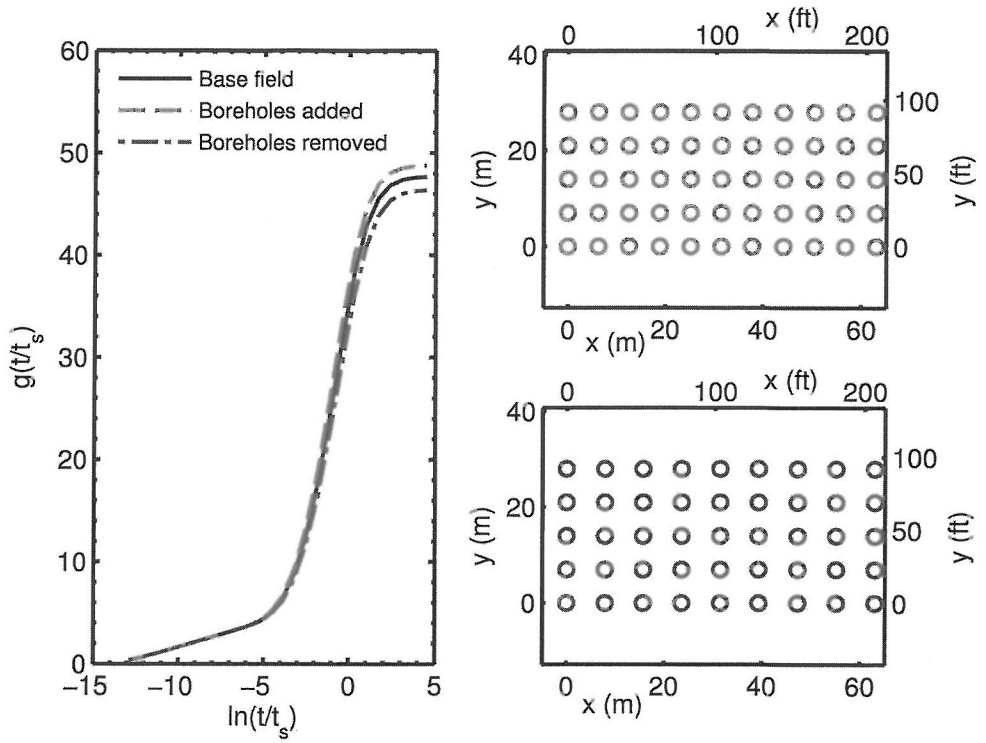

Figure 10 *g-function of a 5 × 10 bore field compared with the g-functions of a 5 × 11 and a 5 × 9 bore field.*

Table 2. Required Borehole Length of the Bore Fields and Relative Change of the Total Required Length

Strategy	3 × 7 Bore Field			5 × 10 Bore Field		
	Required Length, m (ft)	Total Length, m (ft)	Relative Change*	Required Length, m (ft)	Total Length, m (ft)	Relative Change*
Base	121 (397)	2541 (8337)	0	113 (371)	5650 (18,537)	0
Displacing away from center	121 (397)	2541 (8337)	0	113 (371)	5650 (18,537)	0
Displacing towards center	122 (400)	2562 (8406)	+0.8%	114 (374)	5700 (18,701)	+0.9%
Removing boreholes	138 (453)	2484 (8150)	–2.2%	123 (404)	5535 (18,159)	–2.0%
Adding boreholes	108 (354)	2592 (8504)	+2.0%	105 (344)	5775 (18,947)	+2.2%

*Relative to the base configuration. For R_b = 0.1 m·K/W (0.0144 h·ft²·°F/Btu·in.), $\dot{m}$ = 7 L/s (111 gpm) for the 3 × 7 bore field and $\dot{m}$ = 16 L/s (254 gpm) for the 5 × 10 bore field.

The variation of the required borehole length as a result of each strategy is also studied for varying ground thermal properties. Table 4 shows the required individual and total borehole lengths of the 3 × 7 bore field for ground thermal conductivities of 1.7 W/m·K (0.98 Btu/h·ft·°F), 2.0 W/m·K (1.16 Btu/h·ft·°F), and 2.3 W/m·K (1.33 Btu/h·ft·°F). Table 5 shows the required individual and total borehole lengths of the 3 × 7 bore field for ground thermal diffusivities of 0.5×10^6 m²/s (0.54×10^5 ft²/s), 1.0×10^6 m²/s (1.08×10^5 ft²/s), and 1.5×10^6 m²/s (1.61×10^5 ft²/s). The results are similar to the results of Table 2: displacing the boreholes does not reduce the required borehole length significantly and a reduction of the total required length is obtained only when removing boreholes from the bore field. The relative change in the total required length is greater with lower ground thermal conductivity and higher ground thermal diffusivity.

Table 3. g-Function Values at t = 20 Years and Relative Change with the Base Configuration

Strategy	3 × 7 bore field			5 × 10 bore field		
	g-function at t = 20 years	Relative Change*	Relative Change in Required Length*	g-function at t = 20 years	Relative Change*	Relative Change in Required Length*
Base	19.8	0	0	27.5	0	0
Displacing away from center	19.7	–0.5%	0	27.3	–0.5%	0
Displacing towards center	20.1	+1.7%	+0.8%	27.7	+0.7%	+0.9%
Removing boreholes	17.8	–10%	–2.2%	25.6	–6.9%	–2.0%
Adding boreholes	21.6	+9.4%	+2.0%	29.3	+6.5%	+2.2%

*Relative to the base configuration. For R_b = 0.1 m·K/W (0.0144 h·ft²·°F/Btu·in.), $\dot{m}$ = 7 L/s (111 gpm) for the 3 × 7 bore field and $\dot{m}$ = 16 L/s (254 gpm) for the 5 × 10 bore field.

Table 4. Required Borehole Length of the Bore Fields and Relative Change of the Total Required Length for Varying Ground Thermal Conductivity

	k_s = 1.7 W/m·K (0.98 Btu/h·ft·°F)			k_s = 2 W/m·K (1.16 Btu/h·ft·°F)			k_s = 2.3 W/m·K (1.33 Btu/h·ft·°F)		
	Required Length, m (ft)	Total Length, m (ft)	Relative Change*	Required Length, m (ft)	Total Length, m (ft)	Relative Change*	Required Length, m (ft)	Total Length, m (ft)	Relative Change*
Base	136 (446)	2856 (9370)	0	121 (397)	2541 (8337)	0	110 (361)	2310 (7579)	0
Displacing away from center	137 (449)	2877 (9439)	+0.7%	121 (397)	2541 (8337)	0	110 (361)	2310 (7579)	0
Displacing towards center	138 (453)	2898 (9508)	+1.5%	122 (400)	2562 (8406)	+0.8%	111 (364)	2331 (7648)	+0.9%
Removing boreholes	155 (509)	2790 (9154)	–2.3%	138 (453)	2484 (8150)	–2.2%	126 (413)	2268 (7441)	–1.8%
Adding boreholes	122 (400)	2928 (9606)	+2.5%	108 (354)	2592 (8504)	+2.0%	98 (322)	2352 (7717)	+1.8%

*Relative to the base configuration. For R_b = 0.1 m·K/W (0.0144 h·ft²·°F/Btu·in.), $\dot{m}$ = 7 L/s (111 gpm), α_s = 1.0 × 10⁻⁶ m²/s (1.08 × 10⁻⁵ ft²/s).

DISCUSSION

g-Functions

The present study shows that the g-function is a useful tool for the comparison of bore field configurations. In all presented cases, an increase of the g-function caused an increase of the total required length while a reduction of the g-function caused a reduction of the total required length. g-functions can thus be used in early design stages to compare different bore field layouts and select the most promising designs. Simulation of the system is still required to identify the required borehole length.

Practical Limit of the Strategies

The present study analyzed the effects of adding and removing boreholes on the total required borehole length. It was shown that removing boreholes reduces the total required borehole length but increased the individual borehole length. In practice, there are technical and economical limits to the length of a borehole. This limits the number of boreholes that can be removed from a bore field. In general, to reduce the total required borehole length, a bore field should have the least possible amount of boreholes covering the available land area.

Table 5. Required Borehole Length of the Bore Fields and Relative Change of the Total Required Length for Varying Ground Thermal Diffusivity

	$\alpha_s = 0.5 \times 10^{-6}$ m²/s (0.54×10^5 ft²/s)			$\alpha_s = 1.0 \times 10^{-6}$ m²/s (1.08×10^5 ft²/s)			$\alpha_s = 1.5 \times 10^{-6}$ m²/s (1.61×10^5 ft²/s)		
	Required Length, m (ft)	Total Length, m (ft)	Relative Change*	Required Length, m (ft)	Total Length, m (ft)	Relative Change*	Required Length, m (ft)	Total Length, m (ft)	Relative Change*
Base	106 (348)	2226 (7303)	0	121 (397)	2541 (8337)	0	131 (430)	2751 (9026)	0
Displacing away from center	106 (348)	2226 (7303)	0	121 (397)	2541 (8337)	0	131 (430)	2751 (9026)	0
Displacing towards center	107 (351)	2247 (7372)	+0.9%	122 (400)	2562 (8406)	+0.8%	132 (433)	2772 (9094)	+0.8%
Removing boreholes	122 (400)	2196 (7205)	–1.3%	138 (453)	2484 (8150)	–2.2%	148 (486)	2664 (8740)	–3.2%
Adding boreholes	95 (312)	2280 (7480)	+2.4%	108 (354)	2592 (8504)	+2.0%	117 (384)	2808 (9213)	+2.1%

*Relative to the base configuration. For $R_b = 0.1$ m·K/W (0.0144 h·ft²·°F/Btu·in.), $\dot{m} = 7$ L/s (111 gpm), $k_s = 2.0$ W/m·K (1.16 Btu/h·ft·°F).

CONCLUSION

A model of the thermal response of bore fields (Cimmino et al. 2013) is adapted for the simulation of GSHP systems. The model accounts for thermal interactions among boreholes by imposing a borehole wall temperature equal for all boreholes. The model is used to produce g-functions for fields of 21 (3 × 7) and 50 (5 × 10) boreholes and simulate the bore fields to obtain the total required borehole length for each field.

Four strategies, consisting in displacing boreholes away or towards the center of the bore field and adding or removing boreholes from the bore field, are tested to study their impact on the total required borehole length. It is shown that removing boreholes from the bore fields leads to a reduction of the total required length and adding boreholes increases the total required length. Displacing boreholes inside the bore field has a relatively small impact on the total required length. Removing three boreholes from the 3 × 7 bore field led to a reduction of 2.2% of the total required length, but increased the individual length of the boreholes by 14.0%. Removing five boreholes from the 5 × 10 bore field led to a reduction of 2.0% of the total required length, but increased the individual length of the boreholes by 8.8%. It was shown that the g-function can be used to identify the configuration with the lowest total required length. Similar results were obtained when using different values of ground thermal conductivity and ground thermal diffusivity. The relative change in the total required length was shown to be greater with lower ground thermal conductivity and higher ground thermal diffusivity.

ACKNOWLEDGMENTS

This work was partly funded by the NSERC Smart Net-Zero Energy Buildings Strategic Research Network (SNEBRN). The authors also wish to thank the Canadian GeoExchange Coalition and ASHRAE for a scholarship and a grant-in-aid awarded to the first author.

NOMENCLATURE

B	=	borehole spacing, m (ft)
c_p	=	fluid thermal capacity, kJ/kg·K (Btu/lb·°F)
D	=	borehole buried depth, m (ft)
f_i	=	bore field form factor for row i
F, F^{-1}	=	direct and inverse Fourier transforms
g	=	g-function
H	=	borehole length, m (ft)
h	=	borehole-to-borehole response factors
k_s	=	ground thermal conductivity, W/m·K (Btu/h·ft·°F)
L, L^{-1}	=	direct and inverse Laplace transforms
$\dot{m}$	=	fluid flow rate, L/s (gpm)
N	=	number of time steps
N_b	=	number of boreholes
Q, Q'	=	heat extraction rate, heat extraction rate per unit borehole length, kW/m (kBtu/h)
q, q'	=	heat extraction rate increment, heat extraction rate increment per unit borehole length, kW/m (kBtu/h)
R_b	=	borehole thermal resistance, mK/W (h·ft²·°F/Btu·in.)
r_b	=	borehole radius, m (in.)
$T, \Delta T$	=	temperature, temperature variation, °C (°F)
$t, \Delta t$	=	time, time-step (s)
t_s	=	bore field characteristic time (s)

Greek Symbols

α_s	=	ground thermal diffusivity, m^2/s (ft^2/s)
σ	=	damping coefficient for the numerical Laplace transform (1/s)
ρ	=	fluid density, kg/m^3 (lb/ft^3)

Subscripts

b	=	borehole wall
g	=	ground
hor	=	horizontal
i	=	borehole i
$i \rightarrow j$	=	from borehole i to borehole j
max	=	maximum
min	=	minimum
out	=	outlet

REFERENCES

Beck, M., P. Bayer, M. de Paly, J. Hechy-Méndez, and A. Zell. 2013. Geometric arrangement and operation mode adjustment in low-enthalpy geothermal borehole fields for heating. *Energy* 49(1):434–43.

Bernier, M.A., P. Pinel, R. Labib, and R. Paillot. 2004. A multiple load aggregation algorithm for annual hourly simulations of GCHP systems. *HVAC&R Research* 10(4):471–87.

Blomberg, T., J. Claesson, P. Eskilson, G. Hellström, and B. Sanner. 2008. *EED 3.0, Earth Energy Designer.* www.buildingphysics.com/manuals/EED3.pdf.

Carslaw, H.S., and J.C. Jaeger. 1946. *Conduction of heat in solids*, 2nd ed. Chapter 13, The Laplace transformation: Problems on the cylinder and sphere. New York: Oxford University.

Cimmino, M., M. Bernier, and P. Pasquier. 2012. Utilisation des g-functions de Eskilson pour la simulation de systèmes géothermiques. *Proceedings of eSim 2012*, 282–95. Halifax, NS, Canada.

Cimmino, M., and M. Bernier. 2013. Preprocessor for the generation of g-functions used in the simulation of geothermal systems. *Proceedings of BS2013*. Chambéry, France.

Cimmino, M., M. Bernier, and F. Adams. 2013. A contribution towards the determination of g-functions using the finite line source. *Applied Thermal Engineering* 51(1–2):401–12.

Cimmino, M., and M. Bernier. 2014. A semi-analytical method to generate g-functions for geothermal bore fields. *International Journal of Heat and Mass Transfer* 70(c):641–50.

Claesson, J., and S. Javed. 2011. An analytical method to calculate borehole fluid temperatures for time-scales from minutes to decades. *ASHRAE Transactions* 117(2):279–88.

Eskilson, P. 1987. Thermal analysis of heat extraction boreholes. PhD Thesis, University of Lund, Lund, Sweden.

Fisher, D.E., S.J. Rees, S.K. Padhmanabhan, and A. Murugappan. 2006. Implementation and validation of ground-source heat pump system models in an integrated building and system simulation environment. *HVAC&R Research* 12(3A):693–710.

Fossa, M. 2011. The temperature penalty approach to the design of borehole heat exchangers for heat pump applications. *Energy and Buildings* 43(6):1473–479. doi: 10.1016/j.enbuild.2011.02.020.

Hellström, G., and B. Sanner. 1994. Software for dimensioning of deep boreholes for heat extraction. *Proceedings of Calorstock 1994*, 195–202. Espoo/Helsinki, Finland.

Huber, A. 2011. *Program EWS: Calculation of Borehole Heat Exchangers*. Zürich, Switzerland.

Ingersoll, L.R., F.T. Adler, H.J. Plass, and A.C. Ingersoll. 1950. Theory of earth heat exchangers for the heat pump. *Heating, Piping & Air Conditioning* 22:113–22.

Ingersoll, L.R., and H.J. Plass. 1948. Theory of the ground pipe heat source for the heat pump. *Heating, Piping & Air Conditioning* 20(119):119–22.

Ingersoll, L.R., O.J. Zobel, and A.C. Ingersoll. 1954. *Heat conduction: With engineering, geological and other applications*, 2nd ed. Theory of earth heat exchanger for the heat pump. New York: McGraw-Hill.

Kurevija, T., D. Vulin, and V. Krapec. 2012. Effect of borehole array geometry and thermal interferences on geothermal heat pump system. *Energy Conversion and Management* 60:134–42.

Lamarche, L. 2009. A fast algorithm for the hourly simulations of ground-source heat pumps using arbitrary response factors. *Renewable Energy* 34(10):2252–2258.

Lamarche, L., and B. Beauchamp. 2007a. A new contribution to the finite line-source model for geothermal boreholes. *Energy and Buildings* 39(2):188–98.

Lamarche, L., and B. Beauchamp. 2007b. A fast algorithm for the simulation of GCHP systems. *ASHRAE Transactions* 113:470–76.

Liu, X. 2005. Development and experimental validation of simulation of hydronic snow melting systems for bridges. PhD Thesis, Oklahoma State University, Stillwater, OK.

Liu, X., and G. Hellstrom. 2006. Enhancements of an integrated simulation tool for ground-source heat pump system design and energy analysis. *Proceedings of the 10th International Conference on Thermal Energy Storage*, NJ: Galloway.

Marcotte, D., and P. Pasquier. 2008. Fast fluid and ground temperature computation for geothermal ground-loop heat exchanger systems. *Geothermics* 37(6):651–65.

Marcotte, D., and P. Pasquier. 2009. The effect of borehole inclination on fluid and ground temperature for GLHE systems. *Geothermics* 38(4):392–98.

Moreno, P., and A. Ramirez. 2008. Implementation of the numerical Laplace transform: A review. *IEEE Transactions on power delivery* 23(4):2599–609.

Robert, F., and L. Gosselin. 2014. New methodology to design ground coupled heat pump systems based on total cost minimization. *Applied Thermal Engineering* 62(2):481–91.

Spitler, J.D. 2000. A design tool for commercial building loop heat exchangers. Presented at the Fourth International Heat Pumps in Cold Climates Conference, Aylmer, Québec, August 17–18, 2000.

Wedepohl, L.M. 1983. Power system transients: Errors incurred in the numerical inversion of the Laplace transforms. *Proceedings of the 26th Midwest Symposium on Circuits and Systems*, 174–78, Puebla, Mexico.

Yavuzturk, C., and J.D. Spitler. 1999. A short time step response factor model for vertical ground loop heat exchangers. *ASHRAE Transactions* 105(2):475–485.

Zeng, H.Y., N.R. Diao, and Z.H. Fang. 2002. A finite line-source model for boreholes in geothermal heat exchangers. *Heat Transfer—Asian Research* 31(7):558–567.

DISCUSSION

José Acuña, Research Engineer, KTH Royal Institute of Technology, Stockholm, Sweden: Would the results be different for other load profiles? How dependent is the result on the load profile? Can you say something about the optimum borehole distance for a balanced load profile?

Massimo Cimmino: The results are mostly dependent on the average annual load imbalance. The variations in total required borehelole length increase for greater annual load imbalances. The optimum borehole distance for balanced load profiles was not studied.